Domain wall fermions in vector gauge theories

T. Blum[a]

[a]Physics Department, Bldg. 510A, Brookhaven National Lab
Upton, NY 11973-5000, USA

I review domain wall fermions in vector gauge theories. Following a brief introduction, the status of lattice calculations using domain wall fermions is presented. I focus on results from QCD, including the light quark masses and spectrum, weak matrix elements, the $n_f = 2$ finite temperature phase transition, and topology and zero modes and conclude with topics for future study.

1. INTRODUCTION

Several years ago Kaplan had the idea for a lattice discretization of the Dirac operator that preserves chiral symmetry at any lattice spacing[1]. This miracle is performed by adding an *odd* infinite dimension to the usual *even* dimensional spacetime. The mass of the fermion is given the shape of a domain wall in this extra dimension. The mass is large, positive on one side of the defect, negative on the other. Chiral zero modes then arise naturally on the wall where the mass is zero. If the extra dimension is periodic, an anti-domain wall appears at the other end of the lattice with a zero mode of the opposite chirality. These two chiral zero modes are coupled to the same (4d) gauge field to simulate a vector gauge theory, like QCD. The chiral symmetry is manifest: the left and right handed fermions have been separated globally in the extra dimension, so they may be rotated independently.

This realization of chiral zero modes was already known to occur in the continuum, for instance, by Callan and Harvey who studied topological defects embedded in higher dimensions[2]. There and in Kaplan's original study one may suppose that the extra 5th dimension is physical: our 4d spacetime is bound to the wall at low energies, but at high enough energies the 5th dimension becomes perceivable. It is interesting to note such ideas have recently been proposed as a natural mechanism for the spontaneous breaking of supersymmetry[3]. Loosely speaking, domain walls are D-branes, and similar models for realistic "compactified" universes have recently been proposed(for example, see Ref. [4]).

Shortly after Kaplan's original proposal and also motivated by an independent proposal by Frolov and Slavnov[5], Naryanan and Neuberger transformed the extra dimension into an infinite flavor space of heavy regulator fields[6]. Using a transfer matrix formalism, the chiral determinant is given as the overlap of the ground states of two Hamiltonians(hence the name, the overlap formulation, or the overlap, for short). The overlap and Kaplan's domain wall fermions(DWF) are equivalent in the particular case where the extra dimension is infinite. The overlap provides an elegant framework for studying the Index theorem on the lattice. It is the starting point for a new lattice Dirac operator that also maintains chiral symmetry on the lattice[7](see below). An extensive review of the overlap is given in Ref. [8].

The original proposal by Kaplan was intended as a lattice chiral gauge theory. However, it was soon recognized that the discretization would be useful for lattice QCD[9] since conventional methods explicitly break chiral symmetry. Recent numerical studies have shown the actual extent of the extra dimension can be modest, 10-20 sites for simulations of quenched QCD, and still preserve the chiral symmetry to a high degree of accuracy[10–12]. Further, DWF are accurate to order $O(a^2)$ since no (mass) dimension five operators that are also chirally symmetric exist to cancel $O(a)$ errors[13,11]. Indeed, the initial numerical results indicate improved scaling. This scaling (if it holds up after further scrutiny) offsets the cost

of the extra dimension.

For a finite extra dimension with N_s sites, the leading discretization errors are expected to be $O(a)\exp(-CN_s)$ where C is the rate of exponential fall off in the extra dimension. This has been verified at one loop in perturbation theory for QCD[14]. In particular, the authors of Ref. [14] calculate the one loop fermion self-energy and find that the mass of the light mode remains exponentially small. Even after accounting for exponentially small terms in the free propagator that were neglected in Ref. [14], Ref. [15] also concludes that the exponential suppression stays intact after one loop radiative corrections.

At this meeting impressive new results were presented for lattice QCD using DWF, including the first dynamical simulations[16]. After a brief description of the method, I focus on the lattice QCD results.

2. BOUNDARY FERMION VARIANT[9]

Shortly after Kaplan's discovery, Shamir reformulated DWF using a lattice in the extra dimension that is half as big. The boundaries of the 5th dimension are explicitly coupled by a small parameter, $-m(m>0)$. We will see that m is proportional to the $4d$ quark mass and receives only multiplicative renormalizations in the limit $N_s \to \infty$. The chiral limit of DWF is thus $N_s \to \infty$ and then $m \to 0$. These features make Shamir's variant of DWF useful for numerical simulations.

The action for DWF is essentially an ordinary 5d Wilson fermion action:

$$\begin{aligned} S_{dwf} &= -\sum_{x,y,s,s'} \bar{\psi}\left(\not{D}_{x,y}\delta_{s,s'} + \not{D}_{s,s'}\delta_{x,y}\right)\psi, \\ \not{D}_{x,y} &= \frac{1}{2}\sum_{\mu}\Big((1+\gamma_\mu)U_{x,\mu}\delta_{x+\hat{\mu},y} \\ &+ (1-\gamma_\mu)U^{\dagger}_{y,\mu}\delta_{x-\hat{\mu},y}\Big) + (M-4)\delta_{x,y}, \\ \not{D}_{s,s'} &= \begin{array}{l} P_R\delta_{1,s'} - mP_L\delta_{N_s-1,s'} - \delta_{0,s'} \\ P_R\delta_{s+1,s'} + P_L\delta_{s-1,s'} - \delta_{s,s'} \\ -mP_R\delta_{0,s'} + P_L\delta_{N_s-2,s'} - \delta_{N_s-1,s'} \end{array}, \end{aligned} \tag{1}$$

where M is the full 5d mass parameter, s and s' denote the extra dimension, and $P_{R,L} = (1 \pm \gamma_5)/2$. There are important differences with the ordinary Wilson action, however. The links in the s direction are set to unity, the relative sign between the Wilson term and the 5d mass term is opposite to the usual convention, and, as mentioned above, the boundaries in the s direction are coupled with a strength m. The boundary conditions are anti-periodic since the Kaplan model is periodic over $2N_s$. Finally, the extra hopping terms have γ_5's in place of γ_μ's; there is no chirality operator in odd dimensions.

In the free theory for $N_s = \infty$ and $p_\mu, m \to 0$ it is straightforward to show that the mass of the light quark is $m_q = mM(2-M)$ and that the singular part of the propagator (on one wall) is

$$G_R(s,s',p) = P_R \frac{M(2-M)}{\not{p} + m_q}(1-M)^{s+s'}. \tag{2}$$

A similar result holds for the other wall. Aside from the extra factor $M(2-M)(1-M)^{s+s'}$, this is same form found in the continuum. The free propagator is exponentially suppressed in the extra dimension with a rate that depends on M. For $M=1$ the mode does not penetrate the extra dimension at all. Note, the doublers have been removed for the choice $0 < M < 2$. As M is increased in increments of two, up to ten, the zero modes disappear from the spectrum and new ones appear, depending on which corners of the Brillouin zone, according to the factor $b(p) = 1 - M + \sum_\mu(1-\cos(p_\mu))$, contribute(see [9] for details). After $M=10$, no zero modes exist. The critical value where the light quark first appears is $M_c = 0$. In Ref. [17], the leading order corrections to the quark mass for finite N_s were given,

$$m_q = M(2-M)(m + (1 - M + O(p^2))^{N_s}). \tag{3}$$

The overlap of the two modes in the extra dimension has generated an exponentially small quark mass. This mass can be made arbitrarily small compared to m by increasing N_s.

In the interacting theory M is additively renormalized, just like ordinary Wilson fermions, $M \to \widetilde{M} = M - M_c$. At one loop, the dominant effect comes from the tadpole diagram which is diagonal in s[14]; hence the above free field results are unchanged up to a simple shift in M. If one uses a

reasonable choice for the coupling constant, then the magnitude of the tadpole contribution agrees nicely with the original nonperturbative estimate (near quenched $\beta \approx 6.0$) for the optimal value of M which minimizes the overlap of the two light modes[10,11]. A similar shift occurs for the dynamical simulations, as well[16]. Eq. (3) also suggests why we do not expect the usual "exceptional" configurations for DWF for *even* N_s: the contribution to m_q is always positive.

Four dimensional quark fields are constructed from the five dimensional fields by taking their chiral projections on the boundaries.

$$\begin{aligned} q_x &= \frac{(1+\gamma_5)}{2}\psi_{x,0} + \frac{(1-\gamma_5)}{2}\psi_{x,N_s-1}, \\ \bar{q}_x &= \bar{\psi}_{x,N_s-1}\frac{(1+\gamma_5)}{2} + \bar{\psi}_{x,0}\frac{(1-\gamma_5)}{2}. \end{aligned} \quad (4)$$

These definitions are the simplest choice for interpolating operators that create and destroy quarks. Other definitions are possible; *i.e.* one may average over some width around each boundary.

Operators constructed from the definitions in Eq. (4) satisfy a set of axial Ward identities[18].

$$\begin{aligned} \Delta_\mu \left\langle A^a_\mu(x)O(y)\right\rangle &= 2m\left\langle J^a_5(x)O(y)\right\rangle \\ &+i\left\langle \delta^a_A O(y)\right\rangle + 2\left\langle J^a_{5q}(x)O(y)\right\rangle . \end{aligned} \quad (5)$$

The identities are derived in the usual way, by demanding invariance of expectation values under infinitesimal transformations. Here, we take advantage of the fact that the left and right handed modes are globally separated in the fifth dimension in order to rotate them independently. The first two terms on the r.h.s appear in the continuum while the last term is "anomalous". For the flavor nonsinglet case it vanishes in the limit $N_s \to \infty$ before the continuum limit is taken[18]. Thus, DWF fermions have the full axial symmetry of the continuum at *any* lattice spacing. However, this does not rule out the possibility that the doublers reappear at strong coupling in order to trivially satisfy Eq. (5). For the singlet case, the last term gives rise to the usual axial anomaly[19].

3. NUMERICAL RESULTS

The first numerical works using DWF for vector gauge theories were studies of the two dimensional vector Schwinger model[20,21]. Both indicated DWF were practical and useful for numerical work. An in-depth study of DWF using the two dimensional vector Schwinger can be found in [17].

The first simulations of QCD using DWF are found in Refs.[10–12]. There it was shown that even modest numbers of sites in the extra dimension were sufficient to maintain the desirable chiral properties of DWF. Within the last year a significant interest in using DWF for QCD has developed, leading to many new results that were presented at this conference. These are described below.

3.1. PCAC Ward identity, zero modes, topology, and finite N_s effects

The anomalous term in Eq. (5) for the PCAC Ward identity ($O = J_5$) can be used to estimate the effect of finite N_s in simulations. Taking the ratio of Eq. (5) with the pseudoscalar correlator leads to $2m + 2\left\langle J_{5q}(x)J_5(y)\right\rangle / \left\langle J_5(x)J_5(y)\right\rangle$ on the r.h.s., so, as long as the second term is small compared to the explicit quark mass m, one expects good chiral behavior.

Results for the relative anomalous contribution are shown in Fig. (1). For $M = 1.7$ all the points are at least an order of magnitude less than the value of $m(0.05)$ used in the simulations, except the point at $N_s = 10$ and $\beta = 5.85$. As shown below, these simulations display good chiral behavior whereas the pion mass, for example, at $\beta = 5.85$ and $N_s = 10$ has a small but non-zero value when extrapolated to $m = 0$. Note also that the effects decrease significantly as the coupling is weakened while the rate appears to increase.

The data in Fig. (1) is plotted on a semi-log plot, so the four points at ($\beta = 5.85$, $M = 1.7$) should lie on a straight line if the suppression of chiral symmetry breaking effects is given by a simple exponential. However, there is noticeable curvature (but, note that the sample of configurations is small). This curvature may indicate power law suppression or exponential suppression with an N_s dependent rate. The latter was observed in the two dimensional vector Schwinger model[17] and was attributed to gauge fields having trivial versus nontrivial topology.

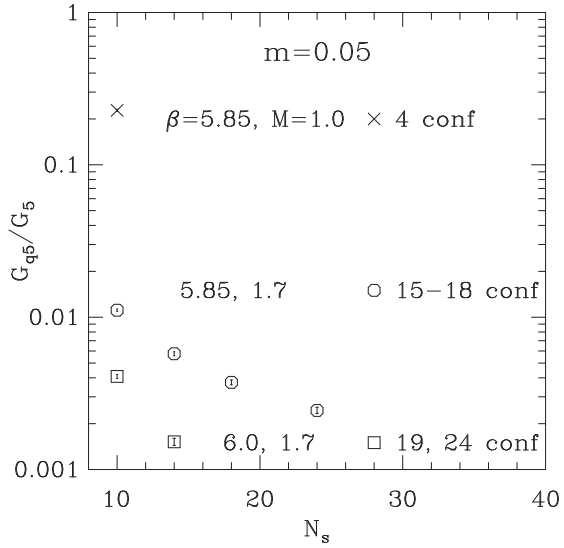

Figure 1. The relative anomalous contribution to the PCAC Ward identity.

The former case may arise from translationally invariant modes in the 5th dimension which are expected to be the dominant anomalous contributions to the Ward identities[18]. Such modes may arise when the 4d Wilson-Dirac operator ($\not{D}_W(-M)$) supports an exact zero mode(here $-M$ refers to supercritical values of the hopping parameter). This is because the spectrum of the Hamiltonian $H_W(-M) \equiv \gamma_5 \not{D}_W(-M)$ defines a transfer matrix for propagation in the 5th dimension[8], $T^{N_s} \equiv \exp(-H_W)^{N_s}$. When $H_W(-M)$ has a zero eigenvalue, T has a unit eigenvalue, and there is no suppression in the extra dimension. There is a gap in the spectrum below the M corresponding to κ_c, which vanishes at κ_c. Naively, the gap is expected to reopen above this value of M[22]. The spectrum of $H_W(-M)$ has been calculated recently[22,23] on quenched configurations corresponding to those in Fig. (1). It was found that $H_W(-M)$ contains many zeroes, or level crossings, arising from lattice instanton-like artifacts, which could close the gap for all values of M suitable for DWF simulations, a disaster.

The data for DWF, on the other hand, are not consistent with this scenario. If there were no suppression, light modes would not be bound to the walls and the ratio of pseudoscalar densities in Fig. (1) would be $O(1)$. However, we have already seen that this ratio is small for $M = 1.7$ which is far from the κ_c region. For $M = 1$ which is near this region at $\beta = 5.85$, the ratio increases dramatically, signalling the absence of light modes. This is consistent with the gap closing at κ_c, as it should. It may be somewhat confusing that the existence of light modes for DWF rules them out for Wilson fermions, and vice-versa.

Translationally invariant modes do exist in DWF simulations, however, so it is important to understand their impact on the 4d physics. In Fig. (2), I show $\bar{\psi}\psi$ as a function of the extra 5th coordinate. The plot is from the Columbia group[24] and is for a single gauge configuration at $\beta = 5.85$. The physical 4d value is at $s = N_s - 1$. $M = 1.45$, which corresponds to an exact zero of H_W. One sees clearly the invariant mode, but its contribution to the physical value of $\bar{\psi}\psi$ is only about one percent. Note, zero modes of $H_W(-M)$ are not zeroes of DWF. In fact, these modes may be quite heavy; since mixing between the modes on opposite walls is maximal in this case, the induced mass may be large.

The Columbia group has also calculated $\langle\bar{\psi}\psi\rangle$ on an ensemble of 200 gauge fields at quenched $\beta = 5.85$[25]. In Fig. (3) a divergence as $m \to 0$ is clearly evident. The divergence arises in the ensemble average from zero modes that are unsuppressed by the (missing) fermion determinant. This has not been seen in lattice simulations until now, presumably due to lattice artifacts. The coefficient of the $1/m$ term should decrease by $1/\sqrt{V}$. The results in Fig. (3) are for $V = 8^3$. The $1/m$ term decreases by a factor of six on a $V = 16^3$ lattice. The Columbia group is currently running on a still larger lattice to resolve this volume dependence.

Finally, the Argonne group has been calculating the low lying spectrum of $R\gamma_5 D_{dwf}$ in order to study the behavior of flavor singlet correlation functions and the restoration of the $U(1)$ axial symmetry above the chiral symmetry phase transition[26]. A sample of their results is shown in

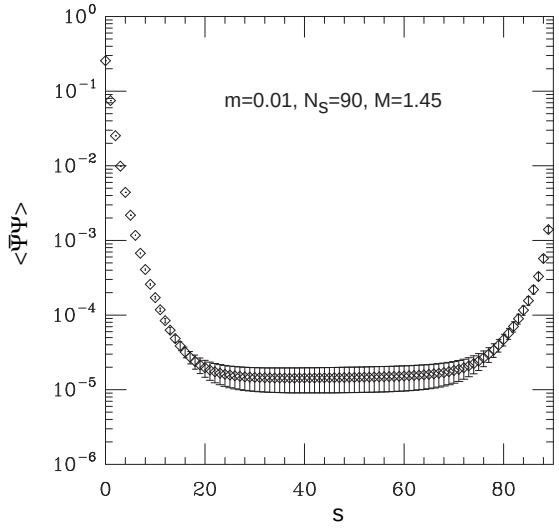

Figure 2. $\bar{\psi}\psi$ as a function of the extra coordinate s on a single quenched configuration at $\beta = 5.85$ from the Columbia group[24]. The value of M corresponds to a zero mode of $H_W(-M)$. The physical value is on the boundary, $s = N_s - 1$.

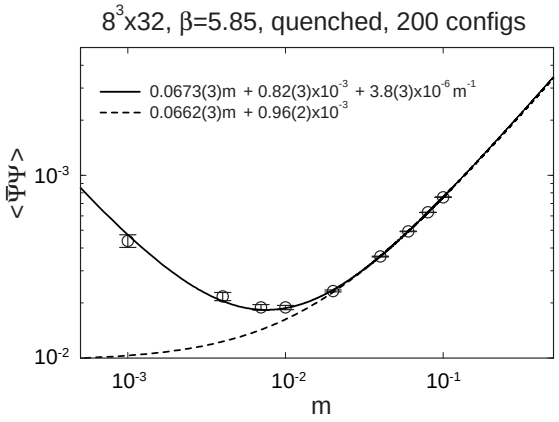

Figure 3. $\langle\bar{\psi}\psi\rangle$ from the Columbia group[25] as a function of the quark mass. The presence of unsuppressed zero modes gives rise to a divergence as $m \to 0$.

Fig. (4) for quenched $\beta = 6.2$. Similar results hold at $\beta = 6.0$. Note that $N_s \leq 10$ in the figure. The lowest eigenvalue is clearly exponential in N_s while the next lowest is N_s independent. For configurations with a net number of instantons, they find the same number of exponentially small eigenvalues, in accord with the Atiyah-Singer Index theorem. They explicitly calculate the topological charge $Q_{top} \equiv m \int d^4x \bar{q}_x \gamma_5 q_x$ (Fig. (5)) and find that it is integer valued within small errors, an impressive result considering the values of N_s used. The deviation of Q_{top} near the origin is a finite N_s effect. Strictly speaking, the Index theorem for DWF is only exact in the limit $N_s \to \infty$. Away from the continuum DWF(and the overlap) do not have a unique index; it depends on M(see Ref. [27], for example).

Thus, I conclude that the gap in $H_W(-M)$ is not actually closed for DWF simulations at values of the coupling used in current simulations. Instead, DWF simply support a number of zero modes corresponding to the *net* number of crossings in the spectrum of H_W below a chosen value of M, as they should. In the ensemble average and $V \to \infty$, as long as the density of exact zero modes of H_W is vanishingly small for a particular M, then M is suitable for DWF simulations.

There is a trend for the suppression to weaken as β decreases(see Fig. (1)). In Ref. [12] it was found that $N_s = 18$ for $\beta = 5.85$ was necessary for the pion mass to extrapolate to zero within statistical errors compared to $N_s = 10$ at 6.0. At 5.7 the Columbia group found that even for $N_s = 48$, the pion mass has a significant intercept at $m = 0$[24]. However, it is not clear that this is entirely a finite N_s effect since results from $N_s = 24$ are roughly the same. The intercept may be related to unsuppressed zero modes from quenching. Our experience has been that at strong couplings there is a minimum value of N_s as well, and tuning M does not have a large effect. The above behavior may be related to an Aoki phase of Wilson fermions at strong coupling[28].

3.2. Light quark masses and spectrum

The quenched QCD pseudoscalar spectrum using DWF was first studied in Refs.[10–12], along with rough estimates for the vector channel. These measurements have also been used to calculate the strange quark mass which was presented

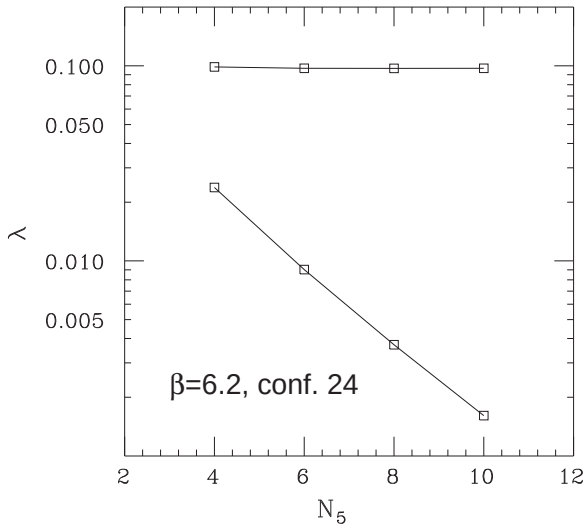

Figure 4. Eigenvalues of the hermitian DWF operator vs. N_s on a configuration with $Q_{top} = 1$. The plot is from the Argonne group[26].

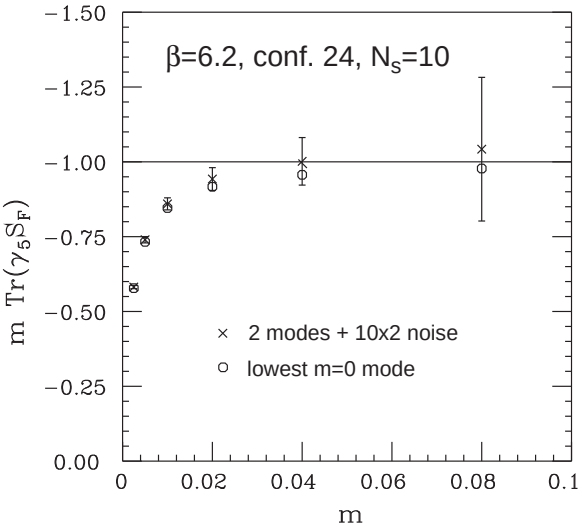

Figure 5. The topological charge Q_{top} from the Argonne group, Ref. [26], on a single configuration with one anti-instanton.

at this conference[29]. The Columbia collaboration presented quenched results for the light pseudoscalar, vector, and nucleon channels at $\beta = 5.7$, as well as the chiral condensate.

In Fig. (6) the pion mass squared is plotted as a function of m for $1.5 \leq M \leq 2.1$ at $\beta = 6.0$. Each curve linearly extrapolates to zero, in accord with lowest order chiral perturbation theory. Fig. (7) shows the same data versus M. m_π^2 has the characteristic quadratic shape expected from free field theory but with a maximum that is shifted from its tree level value. From the figure the shift is approximately 0.8, in good agreement with the estimates of M_c above. The dashed lines correspond to fits to Eq. (3) with M_c fixed to the value corresponding to κ_c for Wilson fermions(see Ref. [29] for details).

The vector and nucleon masses from the Columbia group are shown in Fig. (8). The quenched coupling is 5.7 and the lattice volume is $8^3 \times 32 \times 48$, so these correspond to roughly the same physical volume as the above(in fact, the rho mass scales within errors with the result in Ref. [12]). From their fits, $m_{nuc}/m_\rho \approx 1.4$ in the limit $m = 0$ compared to roughly 1.5 calculated using Kogut-Susskind quarks at the same physical volume[30]. As mentioned above, the chiral symmetry breaking effects due to finite N_s are larger at stronger coupling, so the Columbia group has used $N_s = 48$. Even so, the pion mass is not zero in the limit $m = 0$, but corresponds to roughly 230 MeV.

The Columbia group has calculated $\langle\bar{\psi}\psi\rangle$ for several values of M at quenched $\beta = 5.85$ (Fig. (9)) which yields a clear demonstration of the flavor structure of DWF[24]. Recall that in the free theory we had one flavor for $0 < M < 2$, four flavors for $2 < M < 4$, and so on. A similar pattern emerges nonperturbatively, once again shifted to larger M. The light quark $\langle\bar{\psi}\psi\rangle$ first becomes non-zero at M_c, flattens out in the region $1.65 \lesssim M \lesssim 2.15$, rises rapidly again, and turns over at about 3.4. The first region corresponds to one flavor and the second, four. The ratio of $\langle\bar{\psi}\psi\rangle$ in the two regions is numerically close to four. In the free theory the regions are quadratic polynomials with zeroes at $0, 2, 4, \ldots, 10$. Note that the results become N_s independent at $N_s = 24$.

A first estimate of the (quenched) strange quark mass was presented at the meeting[29].

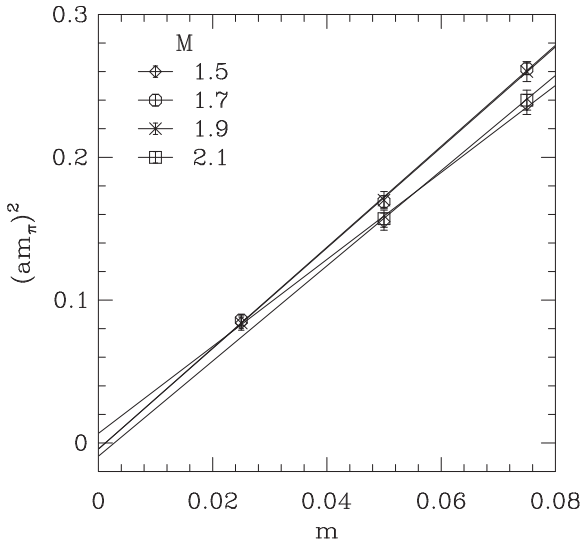

Figure 6. The pion mass squared as a function of the quark mass. $N_s = 14$, $\beta = 6.0$.

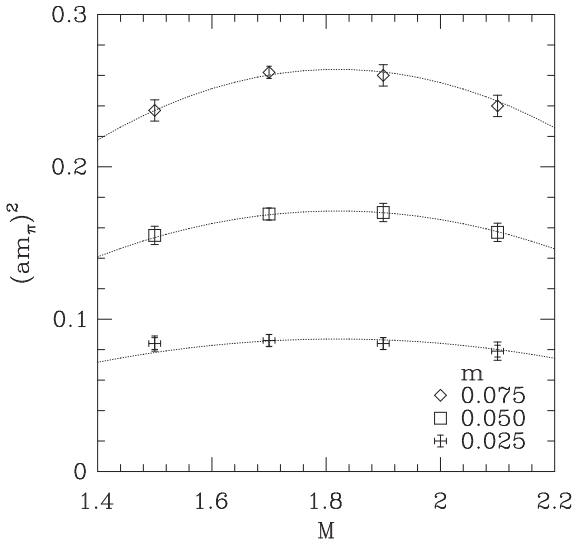

Figure 7. The pion mass squared as a function of the domain wall height. The plot is from Ref. [29]. The dashed lines correspond to fits to Eq. (3) using $\widetilde{M}$ and the nonperturbative value of M_c.

The $\mu = 2$GeV result is compared to conventional determinations in Fig. (10), where one sees rough agreement. The DWF result also appears to scale nicely with the lattice spacing, albeit within rather large statistical errors. A weighted average gives $m_s = 82(15)$MeV.

To get m_s, several steps are needed. First m is tuned in the usual way to yield the kaon mass. To match the DWF result with a continuum scheme, the one loop self-energy calculation of Aoki and Taniguchi was extended to the massive case, $m \neq 0$. One must determine a value for $\widetilde{M} = M - M_c$ to stick into the one loop analog of Eq. (3). In the above it was determined from κ_c. This method is not exact, even though it is nonperturbative. That is because of the symmetry of the action under the change $M \to 10 - M$; $M = 5$ is a fixed point so M is not shifted uniformly. While a more accurate determination of $\widetilde{M}$ is desirable, simply using κ_c only introduces a small error in the final value of $\widetilde{M}(2-\widetilde{M})$[1]. Ultimately, the best solution is to calculate the quark mass renormalization Z_m nonperturbatively (using the method of [31], for instance), where this extra factor is taken into account automatically.

[1] I thank Y. Shamir for pointing this out.

3.3. Weak interaction matrix elements

The study of weak interaction matrix elements was one of the original motivations for using DWF for QCD simulations[10,11]. This is because the matrix elements of many important weak operators between pseudoscalar states vanish linearly with the quark mass, which is a direct consequence of chiral symmetry[32]. Ordinary Wilson quarks explicitly break chiral symmetry, so the naive lattice transcription of these operators does not vanish in the chiral limit. This is a well known, long standing problem. In principle, the solution is to fine tune the continuum-like operators with others that transform under different chiral representations to restore the correct behavior in the chiral limit. Alternatively, one may use Kogut-Susskind quarks which do exhibit the correct behavior since they maintain an exact abelian axial symmetry on the lattice. This rem-

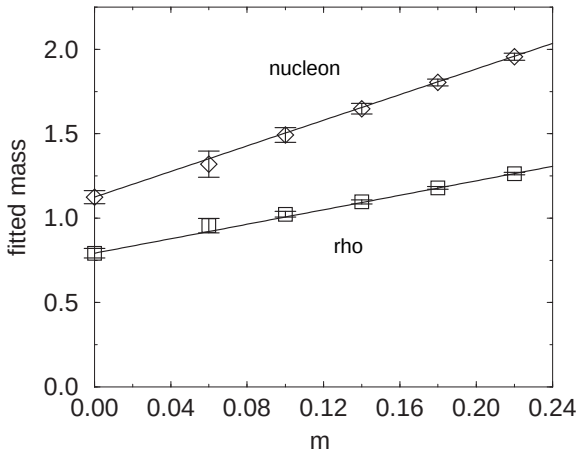

Figure 8. The vector and nucleon masses as a function of m. The plot is from Ref. [24].

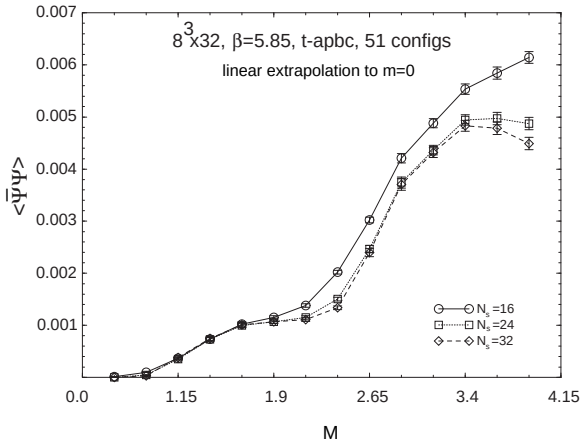

Figure 9. $\langle\bar{\psi}\psi\rangle$ as a function of M from Ref. [24].

nant of the continuum is enough to ensure the proper behavior. However, the price of Kogut-Susskind quarks is the breaking of the continuum flavor symmetries which induces significant lattice artifacts. As we shall see, DWF seem to have significantly smaller discretization errors than the Kogut-Susskind variety.

The vanishing of weak matrix elements in the chiral limit is a stringent test of the chiral symmetry of DWF since even with operator (un)mixing this is a difficult achievement (see Refs.[35,33] for recent results with nonperturbative and perturbative mixing, respectively). Fig. (11) shows the matrix element of the left-left weak operator ($O_{LL} = (\bar{s}\gamma_\mu(1-\gamma_5)d)^2$) that describes $K^0 - \bar{K}^0$ mixing. For all three values of β, 5.85, 6.0, and 6.3, it vanishes linearly with m, as it should according to chiral perturbation theory[32].

The matrix element of O_{LL} is conventionally normalized to its value in the vacuum saturation approximation which yields the B parameter. The kaon B parameter, B_K, is an important phenomenological parameter used to extract part of the CKM matrix from experimental measurements, which in turn constrains the Standard Model. The quenched DWF result is shown for several lattice spacings in Fig. (12). The impressive Kogut-Susskind result of Ref. [36] is shown for comparison. Since O_{LL} is generated by the operator product expansion, it is scale dependent, and therefore the result at each coupling must be run to a common scale before the continuum limit is taken. In the continuum, the vacuum saturated value of $\langle K^0|O_{LL}|\bar{K}^0\rangle$ is proportional to the square of the axial current matrix element which does not get renormalized since the axial current is partially conserved. As explained above, DWF have a partially conserved axial current, but this is not the current that is needed for the vacuum saturation of O_{LL} on the lattice since we have chosen to construct O_{LL} from the quark operators defined in Eq. (4). Therefore, the denominator in B_K also receives a (finite) multiplicative renormalization. Since these renormalizations have not yet been done for DWF, the most that can be said is that the result for B_K is consistent with the Kogut-Susskind result. Nevertheless, the indication from Fig. (12) is that discretization errors are significantly smaller in the DWF case. Needless to say, it is a high priority to reduce the statistical errors and determine the renormalization factors in order to precisely determine the lattice spacing dependence. It is important to point out that the lattice volumes of the last two Kogut-Susskind points in Fig. (12) are $56^3 \times 96$ and $48^3 \times 96$ and correspond to physical volumes of 2.3fm^3 and 2.8fm^3, respectively. If the improved

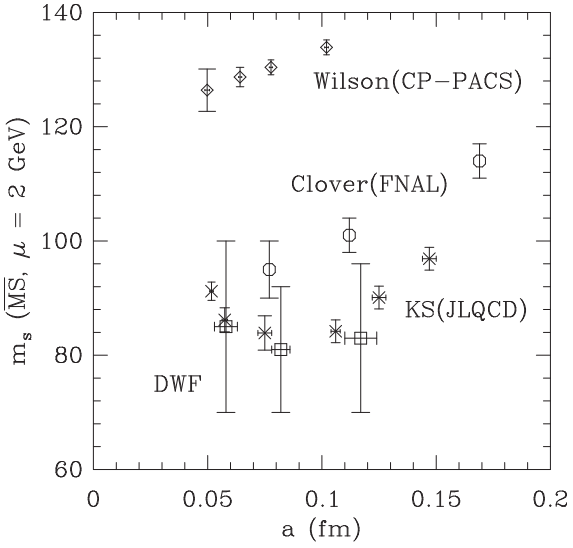

Figure 10. The strange quark mass from Ref. [29] after matching to the $\overline{\rm MS}$ scheme.

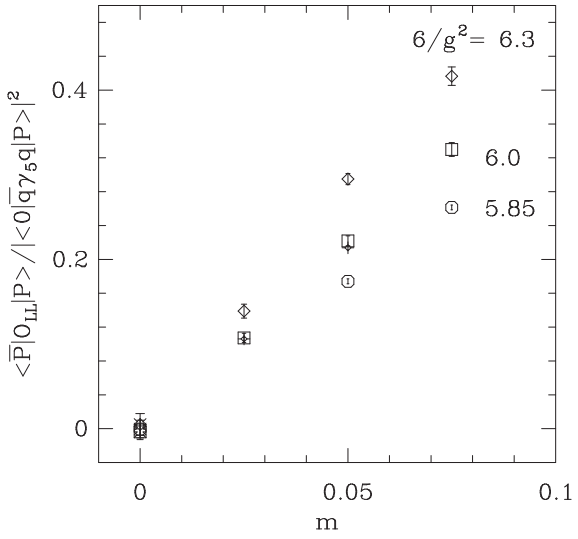

Figure 11. The matrix element of O_{LL} between degenerate pseudoscalar states. It vanishes in the chiral limit, a stringent test for the chiral symmetry properties of DWF.

scaling of DWF holds up, then the added cost of the extra dimension will be significantly offset by the smaller $4d$ lattice volumes allowed by larger lattice spacings.

At $\beta = 6.0$, there is also a value of B_K on a $24^3 \times 40$ lattice which indicates that finite volume effects are not large.

Encouraged by the results of our B_K calculation, we have begun calculations of the $\Delta s = 1$ effective weak Hamiltonian operators that govern $K \to \pi\pi$ decays and are necessary for ϵ'/ϵ and the $\Delta I = 1/2$ rule, for example[34]. Once again, in the continuum, chiral symmetry restricts the behavior of these operators and is therefore important for the lattice calculations as well. In fact, the good chiral properties of DWF allow the use of the method of Bernard, *et al.* [32] to calculate unphysical $K \to \pi$ amplitudes and relate them, using chiral perturbation theory, to the physical $K \to \pi\pi$ amplitudes. The unphysical three point functions are easier to calculate on the lattice. Kilcup and Pekurovsky are using the same method with Kogut-Susskind quarks to calculate these amplitudes[37]. There it is already clear that perturbation theory fails for the renormalization of these operators, and a nonperturbative method is needed. On the other hand, since the one-loop renormalization of the DWF quark mass is reasonable, it is still possible to renormalize the DWF operators perturbatively.

Our preliminary results on an ensemble of eighteen gauge configurations at $\beta = 6.0$ are shown in Fig. (13). The lattice volume is $24^3 \times 40 \times 10$. As is well known, these amplitudes are more difficult to calculate than O_{LL} because of the notorious "eye" contractions which occur since a quark and an antiquark with the same flavor in the operator can annihilate each other. In order to efficiently average the operator over all spatial sites on a fixed time slice, one uses a random source(s) on the time slice. The results shown in Fig. (13) are for a single random source in the middle of the lattice. It is therefore encouraging to see a signal at all. $O_1, \ldots, O_6$ which transform under (8,1) representations of $SU(3)_L \times SU(3)_R$ should vanish linearly in the chiral limit. O_5 and

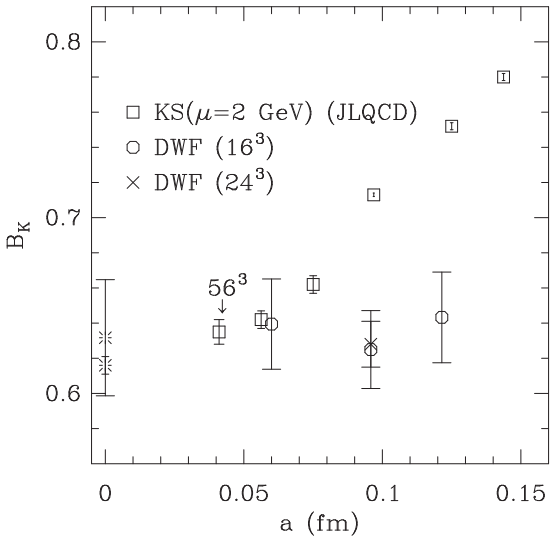

Figure 12. The kaon B parameter. The Kogut-Susskind result is from Ref. [36]. DWF indicate improved scaling in this case.

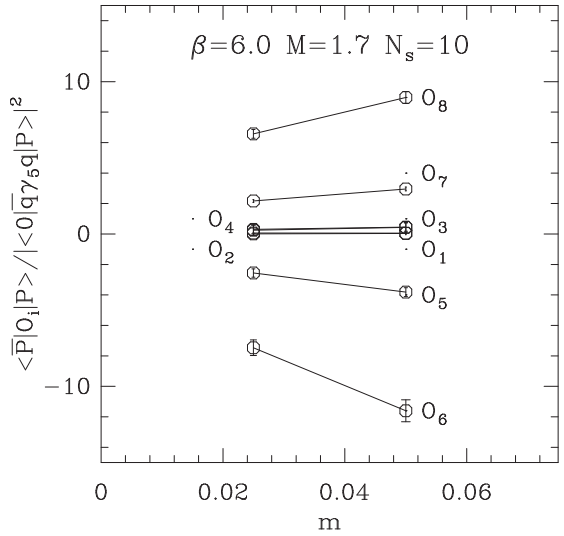

Figure 13. $K \to \pi$ matrix elements of the $\Delta s = 1$ effective weak Hamiltonian.

O_6 do not, though they miss the origin by less than two standard deviations. This could be due to the small statistics of our ensemble, or that $N_s = 10$ is not large enough. Also note that there are only two quark masses, and the random source was different for each. $O_{7,8}$ transform under (8,8) representations so do not vanish in the chiral limit[32]. $O_{5,\ldots,8}$ are expected to be larger than $O_{1,\ldots,4}$ since they are left-right operators which is the case here, and the color mixed operators are roughly three times their unmixed counterparts, as expected from the vacuum saturation approximation.

In order to carry the above through to the physical $K \to \pi\pi$ decays, an important vacuum subtraction, $\langle K|O_i|0\rangle$ must still be made[32].

3.4. Dynamical simulations and non-zero temperature

The Columbia group has begun the first simulations using dynamical DWF to study the two flavor QCD chiral symmetry restoration phase transition at non-zero temperature. These simulations are obviously quite demanding. Impressive preliminary results were presented at this conference[16]. They, as well as the Argonne group also presented quenched and semi-classical results related to the anomalous $U(1)$ axial symmetry[38,25,26]. A detailed description of the Columbia group's semi-classical results can be found in Ref. [39].

Using DWF, the two flavor chiral phase transition in QCD appears qualitatively similar to the Kogut-Susskind result. In Fig. (14) there is a smooth crossover in both the Polyakov loop and $\langle\bar{\psi}\psi\rangle$ starting at $\beta \approx 5.2$ ($N_\tau = 4$). In the limit $m \to 0$, below the transition $\langle\bar{\psi}\psi\rangle$ is spontaneously broken while above the transition chiral symmetry is restored (Fig. (15)). The very small but statistically significant non-zero intercept in Fig. (15) is presumably due to finite N_s effects. From Fig. (15) ordinary finite volume effects are small as well. While these results are very encouraging, the quark masses are still too heavy to discuss details like the order of the transition and critical exponents. It should be stressed that for the first time the correct number of light pi-

ons is being simulated in dynamical studies of the $n_f = 2$ QCD chiral phase transition, which may be crucial to the dynamics.

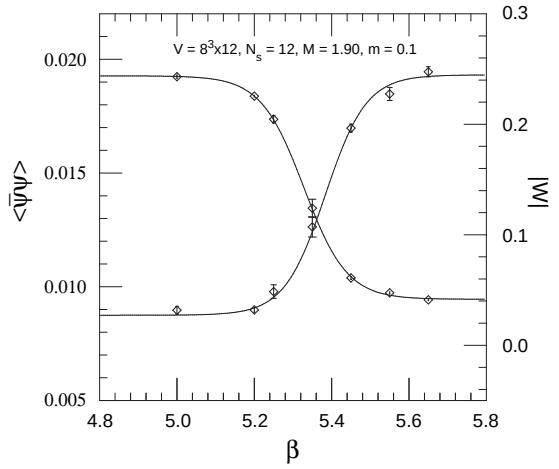

Figure 14. $\langle\bar{\psi}\psi\rangle$ and the Polyakov loop for $n_f = 2$ from the Columbia collaboration[16]. Both exhibit a rapid crossover near $\beta = 5.4$.

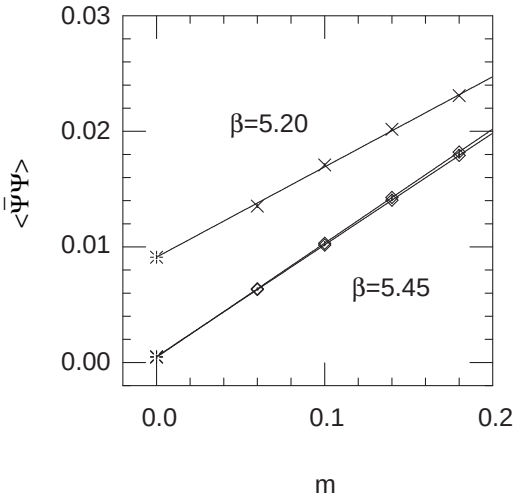

Figure 15. $\langle\bar{\psi}\psi\rangle$ as a function of m for $\beta = 5.20$(upper curve) and 5.45(lower curves). Chiral symmetry is restored above the phase transition. The two lower curves correspond to 8^3 and 16^3 lattices. $n_f = 2$. The plot is from the Columbia group Ref. [16].

The pseudo-critical coupling is a function of M(Fig. (16)). There are two reasons for this: the quark mass depends on M (Eq. (3)), and the number of flavors is a function of M. Below M_c there are no light states bound to the domain wall. At M_c the domain wall states just begin to form so β_c starts at its quenched value. As M increases, a full range of momenta are available to the states on the walls and β_c decreases to its $n_f = 2$ value(remember that the fermion determinant is $D^\dagger D$). As M increases still further, four light quarks eventually appear on the domain walls so β_c decreases to its $n_f = 8$ value.

Both the Argonne and Columbia groups have studied the restoration of the $U(1)_A$ symmetry above the chiral phase transition. As mentioned earlier, the Argonne group has measured the topological charge(see Fig. (5)) on quenched configurations, but have not yet published their results for flavor singlet meson masses, correlators, or susceptibilities. The Columbia group has measured $n_f = 2$ screening masses for the pion and the delta which should be degenerate if the $U(1)_A$ symmetry is restored. The mass difference somewhat above the chiral transition is shown in Fig. (17). There is a small but significant value at $m = 0$. Note the data appears quadratic in m, as expected, due to the restoration of chiral symmetry. There are no known lattice artifacts present to obscure this picture as is the case for Kogut-Susskind quarks.

In general, dynamical simulations require a Pauli-Villars(PV) subtraction. The action for the $N_s - 1$ heavy states induced by the extra dimension dominates the total action in the limit $N_s \to \infty$[6]. The form of the subtraction is not unique; a second order operator is suggested in Ref. [9] while in Ref. [17,16] a first order operator is used. The latter version is vulnerable to the "exceptional" configurations discussed in section 3.1. That is, if $D_W(-M)$ supports an exact zero mode, so does the first order operator, which has periodic instead of anti-periodic boundary condi-

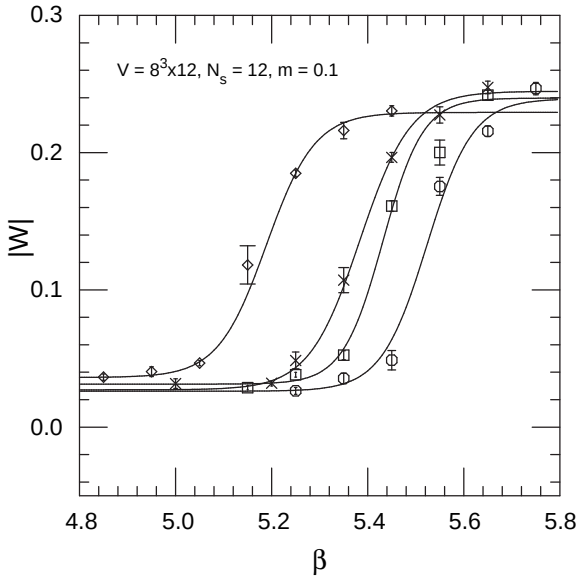

Figure 16. The Polyakov loop from Ref. [16] for several values of M. $n_f = 2$. The pseudo-critical coupling depends on the choice of M.

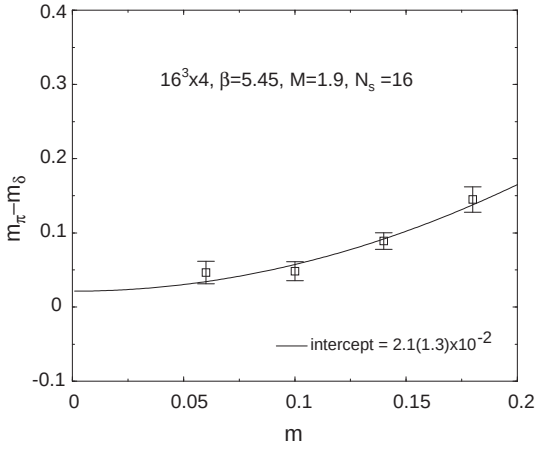

Figure 17. The difference in screening masses above the chiral symmetry restoration phase transition from Ref. [16]. $n_f = 2$. A difference of zero at $m = 0$ indicates restoration of the $U(1)_A$ symmetry.

tions in the extra dimension. This zero mode is not canceled by a corresponding massless mode in the DWF operator. On the other hand, the authors of Ref. [16] have seen no evidence for these modes in their simulations. A method for suppressing such configurations has been suggested in Ref. [40], which is described in the next section.

4. TOPICS FOR FUTURE STUDY

Beyond using DWF in their present form to do useful phenomenology, future studies will focus on improvements that reduce the size of the extra dimension and/or increase the rate of exponential suppression. Several proposals have already been made[41,42,40]. The first proposal uses a hyper-cubic action instead of a Wilson like action. The last two include an explicit lattice spacing in the extra dimension which renders the DWF action positive definite for any gauge coupling. In Ref. [40] it is argued that this restricts eigenvalues of the transfer matrix on the unit circle to the real axis, reducing slowly decaying chiral symmetry violations. There, a modified PV action is considered which suppresses the unwanted zero modes of $D_W(-M)$; an extra term involving the 4d links is added to the PV action to do the job. A side-effect is the small renormalization of the coupling constant.

An exciting development is the related derivation of the overlap-Dirac operator by Neuberger[7]. This lattice discretization, which corresponds to a single massless Dirac particle, is derived from the overlap, but retains no reference to an extra flavor space or dimension. It is completely 4d and has been shown explicitly to satisfy the Ginsparg-Wilson relation[43]. Initial studies indicate the method may be feasible numerically[44–46], though its application to lattice QCD has not yet been demonstrated.

Finally, a new approach to lattice gauge theory is the quantum link model. DWF arise naturally in quantum link models since they are constructed in five dimensions[47].

5. CONCLUSIONS

I have reviewed the present status of DWF for vector gauge theories, in particular QCD. We have seen that DWF with a modest number of sites in the extra dimension maintain their good

chiral properties, which are exact in the limit $N_s \to \infty$. The results show promising behavior in studies where chiral symmetry is important such as weak matrix element phenomenology, dynamical simulations of the chiral symmetry restoration phase transition, and the relation between topology and fermionic zero modes. Indications of improved scaling with DWF need to be verified since this may significantly offset the cost of the added dimension.

I acknowledge many helpful discussions with M. Creutz, R. Mawhinney, Y. Shamir, A. Soni, and M. Wingate. This work was supported by the U.S. DOE, contract DE-AC02-98CH10886. Numerical simulations by the author were done on the NERSC T3E.

REFERENCES

1. D. Kaplan, Phys. Lett. B 288 (1992) 342.
2. C.G. Callan and J.A. Harvey, Nucl. Phys. B 250 (1984) 427.
3. G. Dvali and M. Shifman, Phys. Lett. B 396 (1997) 64; Erratum-ibid. B 407 (1997) 452; G. Dvali and M. Shifman, Nucl. Phys. B504 (1997) 127.
4. R. Sundrum, hep-ph/9807348 and references therein.
5. S.A. Frolov and A.A. Slavnov, Saclay preprint SPhT/92-051 (1992).
6. R. Narayanan and H. Neuberger, Phys. Lett. B 302 (1993) 62.
7. H. Neuberger, Phys. Lett. B 417 141 (1998) 141; H. Neuberger, hep-lat/9807009 and references therein.
8. R. Narayanan and H. Neuberger, Nucl. Phys. B 443 (1995) 305.
9. Y. Shamir, Nucl. Phys. B 406 (1993) 90.
10. T. Blum and A. Soni, Phys. Rev. D 56 (1997) 174.
11. T. Blum and A. Soni, Phys. Rev. Lett. 79 (1997) 3595.
12. T. Blum and A. Soni, hep-lat/9712004.
13. Y. Kikukawa, R. Narayanan, and H. Neuberger, Phys. Lett. B 399 (1997) 105.
14. S. Aoki and Y. Taniguchi, hep-lat/9711004.
15. Y. Kikukawa, H. Neuberger, and A. Yamada, Nucl. Phys. B 526 (1998) 572; H. Neuberger, Phys. Rev. D57 (1998) 5417.
16. P. Vranas this meeting.
17. P. Vranas, Phys. Rev. D57 (1998) 1415.
18. Y. Shamir and V. Furman, Nucl. Phys. B 439 (1995) 54.
19. Y. Shamir, Nucl. Phys. B 417 (1994) 167.
20. A. Jaster, hep-lat/9605011.
21. P. M. Vranas hep-lat/9705023.
22. R. Edwards, U. Heller, and R. Narayanan, hep-lat/9802016.
23. R. Narayanan, plenary talk at this meeting.
24. R. Mawhinney, this meeting.
25. G. Fleming, this meeting.
26. J. Lagae, hep-lat/9809134, this meeting.
27. R. Narayanan and P. Vranas, Nucl. Phys. B 506 (1997) 373.
28. S. Aoki, Nucl. Phys. 60A (Proc. Suppl.) (1998) 206; S. Aoki, T. Kaneda, and A. Ukawa, Phys. Rev. D56 (1997) 1808.
29. M. Wingate, hep-lat/9809065, this meeting.
30. C. Bernard, *et. al.* Nucl. Phys. B60A (Proc. Suppl.) (1998) 249.
31. G. Martinelli, *et al.* , Nucl. Phys. B 445 (1995) 81.
32. C. Bernard, *et al.* , Phys. Rev. D32 (1985) 2343.
33. L. Lellouch, this meeting.
34. M. Ciuchini, *et al.* , Nucl. Phys. B 415 (1994) 403.
35. S. Aoki, *et al.* , Nucl. Phys. B 60A (Proc. Suppl.) (1998) 67.
36. S. Aoki, *et al.* , Phys. Rev. Lett. 80 (1998) 5271.
37. G. Kilcup and D. Pekurovsky, Nucl. Phys. B 63 (Proc. Suppl.) (1998) 293; D. Pekurovsky, hep-lat/9809115, this meeting.
38. A. Kaehler, this meeting.
39. P. Chen, *et al.* , hep-lat/9807029.
40. Y. Shamir, hep-lat/9807012.
41. W. Bietenholtz, hep-lat/9803023.
42. Y. Kikukawa and A. Yamada, hep-lat/9806013.
43. M. Lüscher, Phys. Lett. B 428 (1998) 342.
44. T. Chiu, hep-lat/9804016 and this meeting.
45. H. Neuberger, hep-lat/9806025.
46. R. Edwards, U. Heller, and R. Narayanan, hep-lat/9807017.
47. See U. Wiese, plenary talk, this meeting.